Joint Wide Illumination and Null Insertion Design in RIS-assisted System

Xinyi Lin*, Ziyi Zhou*, Lei Zhang*, Anvar Tukmanov†, Qammer Abbasi*, and Muhammad Ali Imran*
*School of Engineering, University of Glasgow, G12 8QQ, U.K.
†British Telecommunications PLC, Adastral Park, Ipswich, IP5 3RE, U.K.
Email: {x.lin.1, z.zhou.3}@research.gla.ac.uk, {Lei.Zhang, Qammer.Abbasi, Muhammad.Imran}@glasgow.ac.uk, anvar.tukmanov@bt.com

***Abstract*—In this paper, we focus on reconfigurable intelligent surface (RIS)-aided joint wide illumination and null insertion design. This design can be applied in cellular networks, broadcasting, and radar systems, enabling multiple wide null and illumination at arbitrary directions. Our objective is to minimize the deviation between the target pattern and the practical power pattern by designing the passive beamforming at RIS, while the RIS unit modulus weights constraint is illustrated. To tackle the non-convex optimization problem, the low-complexity alternating direction method of multipliers (ADMM) algorithm is proposed. In particular, the augmented objective function is firstly formulated with introduced auxiliary variables, which is then rephrased as a Lagrangian function. By alternatively updating the variables, the objective function converges with the optimized RIS phase shifts. The convergence of simulation results proves the validity of our proposed algorithm, and the proposed algorithm performs quite well in matching the desired and actual power patterns with practical channel model under different number and size of illumination and null areas.**

***Index Terms*—Reconfigurable intelligent surface, least square normalization, passive beamforming.**

I. Introduction

Recently, Reconfigurable Intelligent Surface (RIS) has gained significant attention due to its potential to revolutionize wireless communication systems [1]. Also known as "smart surfaces" [2] or "intelligent reflecting surfaces (IRS)" [3], RIS represents a new paradigm in wireless communications by introducing the concept of actively controlling the propagation of electromagnetic waves in the environment. The RIS is a planar surface that consists of a large number of equal-spaced tunable elements with no RF chain. On one side, by smartly turning the phase shifts of the passive elements, the reflected beam can be adjusted to achieve the desired pattern [4]; on the other side, the implementation of RIS poses no significant cost burden when added to the existing cellular network architecture [5].

As a pivotal and promising technology in shaping the future of wireless communications, RIS has attracted lots of interests across various sectors, including 5G and beyond wireless networks [6], indoor localization [7], Internet of Things (IoT) connectivity [8], and more. Regardless of the considerable benefits of RIS-assisted communication systems, some difficulties still have to be resolved, particularly in the acquisition of full channel state information (CSI). To combat incomplete or inaccurate CSI, the broad beam covering a continuous sector is regarded as a potential solution, as it does not require precise alignment of beams with users or targets. Several relevant research have investigated this technology. Specifically, the authors in [9]–[11] studied the beam broadening techniques in an RIS-assisted system. However, the wide coverage provided by broad beams may unintentionally transmit signals to unintended directions, compromising security, privacy, and cost. The wide null insertion design can be applied to suppress signals towards undesired directions effectively when the directions of interference and blockages are pre-known. Antenna pattern synthesis with multiple discrete and continuous nulls are discussed in [12], [13], where quasi- and mixed-matrix techniques are applied to obtain the beamforming weights. Nevertheless, the proposed beamforming technique is not applicable in RIS-assisted system as it violates the unit modulus constraint of the RIS weights. To the authors' best knowledge, the joint wide coverage and null insertion design remain unexplored in a RIS-assisted system.

Motivated by these facts, in this paper, we propose a joint wide illumination and null insertion design in RIS-assisted system via optimizing the passive beamforming at RIS, given constraints of RIS unit modulus weights. On one side, the wide illumination ensures reliable signal transmission without the accurate CSI of users; on the other side, the extended-null insertion are essential for suppressing signals towards unwanted directions. Instead of using classical semi-definite relaxation (SDR) based method [14], which lifts the problem dimension from N to N^2 and significantly increases the computational complexity [15], a low-complexity alternating direction method of multipliers (ADMM)-based algorithm is proposed in this paper, which effectively address the non-convexity by introducing auxiliary variables. Via alternatively updating RIS phase shifts and the auxiliary variables, a minimized normalization deviation between the target and optimized pattern can be obtained.

The rest of the paper is organized as follows. Section II presents the system model and formulates the optimization problem. Then, Section III introduces the proposed algorithm for pattern synthesis. Simulation results are provided in Section IV to verify the convergence and effectiveness of the proposed ADMM algorithm. Section V concludes the paper.

Notations: Bold-faced upper case letters, bold-faced lower case letters, and light-faced lower case letters denote matrices,

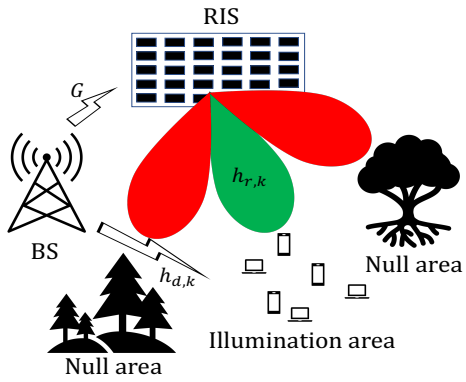

Fig. 1: System model of RIS-assisted joint wide illumination and null insertion design.

column vectors, and scalar quantities, respectively. Superscripts $(\cdot)^T$, $(\cdot)^*$. and $(\cdot)^H$ represent transpose, conjugate, and conjugate-transpose operations, respectively. $\mathcal{R}e\{\cdot\}$ and $\mathcal{I}m\{\cdot\}$ denote the real and imaginary parts of a complex number.

II. System Model

We model a RIS-aided wide illumination and null insertion design as in Fig.1. Specifically, we assume that there are R null areas, where nulls are needed to either combat interference or suppress signals towards blockages and unwanted directions. In addition, there are Q illumination areas, where users with a single antenna are located. Let $\boldsymbol{\theta} = [\theta_1, \theta_2, ..., \theta_M]^H$ denote the RIS phase shift matrix and each element $\theta_m, m = 1, \cdots, M$ in $\boldsymbol{\theta}$ could be expressed as $\theta_m = \beta_m e^{j\alpha_m}$. For maximum reflection efficiency, we let $\beta_m = 1$ and $\alpha_m \in [0, 2\pi]$. Besides, the BS has N elements.

Assume that there are K look-directions across the whole cover domain. Specifically, K_R and K_Q refer to the directions within the null and illumination areas, respectively. We denote $\boldsymbol{h_{d,k}} \in \mathbb{C}^{N\times 1}$, $\boldsymbol{G} \in \mathbb{C}^{M\times N}$, and $\boldsymbol{h_{r,k}} \in \mathbb{C}^{M\times 1}$ as the channel expressions of BS-k-th direction, BS-RIS, and RIS-k-th direction, respectively, where $k \in K$. We further define $\boldsymbol{w} \in \mathbb{C}^{N\times 1}$ as the precoding vector at BS, and $s \in \mathbb{C}$ is the transmit signal with $\mathbb{E}\{ss^*\} = 1$. Then the received signal at the direction k could be expressed as

$$y_k = (\boldsymbol{h_{d,k}^H} + \boldsymbol{h_{r,k}^H}\boldsymbol{\Theta}\boldsymbol{G})\boldsymbol{w}s + n_k, \forall k \in K, \tag{1}$$

where $\boldsymbol{\Theta} = \text{diag}(\boldsymbol{\theta}^T) \in \mathbb{C}^{M\times M}$ and n_k is the additive white Gaussian noise (AWGN) with zero mean and variance σ_n^2, i.e., $n_k \sim \mathcal{CN}(0, \sigma_n^2)$.

We apply the uniform linear array (ULA) configuration to channel vectors, which is generally expressed as

$$\boldsymbol{a}_{\text{ULA}}(\Omega) = [1, e^{j\frac{2\pi f}{c}d\cos\Omega}, \cdots, e^{j\frac{2\pi f}{c}d(N_s-1)\cos\Omega}]^T. \tag{2}$$

We assume that the direct link $\boldsymbol{h_{d,k}}$ follows Rayleigh fading, while RIS-aided channels $\boldsymbol{h_{r,k}}$ and $\boldsymbol{G}$ follow Rician fading. Then $\boldsymbol{h_{d,k}}$, $\boldsymbol{h_{r,k}}$, and $\boldsymbol{G}$ are modeled as

$$\boldsymbol{h_{d,k}} = \text{PL}_{\text{NLOS}}\overline{\boldsymbol{h}}_{\boldsymbol{d}}, \tag{3}$$

$$\boldsymbol{h_{r,k}} = \text{PL}_{\text{LOS},k}(\sqrt{\frac{\varepsilon}{\varepsilon+1}}\boldsymbol{a}(\Omega_{R,k}) + \sqrt{\frac{1}{\varepsilon+1}}\overline{\boldsymbol{h}}_{\boldsymbol{r}}), \tag{4}$$

$$\boldsymbol{G} = \text{PL}_{\text{LOS},0}(\sqrt{\frac{\varepsilon}{\varepsilon+1}}\boldsymbol{a}(\Omega_{R,0})\boldsymbol{a}^T(\Omega_B) + \sqrt{\frac{1}{\varepsilon+1}}\overline{\boldsymbol{G}}). \tag{5}$$

Specifically, PL_{NLOS}, $\text{PL}_{\text{LOS},k}$ and $\text{PL}_{\text{LOS},0}$ denote the corresponding path-loss. ε is the Rician factor. $\Omega_{R,k}$, $\Omega_{R,0}$, and Ω_B denote the departing angle towards the direction k, incident angle at RIS and departing angle at BS towards RIS, respectively. $\overline{\boldsymbol{h}}_{\boldsymbol{d}}$, $\overline{\boldsymbol{h}}_{\boldsymbol{r}}$, and $\overline{\boldsymbol{G}}$ denote the NLOS components of channels, each element of which follows $\mathcal{CN}(0, 1)$.

Additionally, as the direct links is severely blocked and only NLOS paths exist, the channel gain is generally lower than that of the reflective links. We therefore initialize the active beamforming at BS with maximum ratio combining (MRC) for maximal power transmission towards RIS, which can be expressed as $\boldsymbol{w} = \boldsymbol{a}^*(\Omega_B)$. With fixed active beamforming $\boldsymbol{w}$, we rewrite $\hat{h_{d,k}} = \boldsymbol{h_{d,k}}^H\boldsymbol{w}$ and $\hat{\boldsymbol{g}} = \boldsymbol{G}\boldsymbol{w} \in \mathbb{C}^{M\times 1}$, then the beam pattern at the k-th direction in the far field can be expressed as

$$p_k = |\hat{h_{d,k}} + \boldsymbol{h_{r,k}^H}\boldsymbol{\Theta}\hat{\boldsymbol{g}}|. \tag{6}$$

Note that the noise is ignored here as its power is much lower than that of the signal, especially over the time scale.

We further introduce the target pattern $\boldsymbol{t} \in \mathbb{C}^{K\times 1}$ and the weighting factor $\boldsymbol{\kappa} \in \mathbb{C}^{K\times 1}$, which can be designed to assign different weights for different angular regions. Then our proposed design can be interpreted as the following matching problem:

$$\mathbb{P}: \min_{\boldsymbol{\theta}} \quad \|\boldsymbol{\kappa}\cdot(\boldsymbol{t}-\boldsymbol{p})\|_2^2. \tag{7a}$$

$$\text{s.t.} \quad |\theta_m| = 1, m = 1, \cdots, M, \tag{7b}$$

where $\boldsymbol{p} = [p_1, \cdots, p_K]^T$. In the following, we develop the ADMM algorithm to solve the problem $\mathbb{P}$.

III. The Proposed Algorithm for Pattern Synthesis

We firstly combine the RIS-assisted reflective links as $\boldsymbol{\eta}_k = \text{diag}(\boldsymbol{h}_{r,k}^H)\hat{\boldsymbol{g}} \in \mathbb{C}^{M\times 1}$, then the objective function (7a) can be reinterpreted as

$$\min_{\boldsymbol{\theta}} \quad \|\boldsymbol{v} - |\boldsymbol{u} + \boldsymbol{\Lambda}^H\boldsymbol{\theta}|\|_2^2, \tag{8}$$

where $\boldsymbol{u} = [\kappa_1\hat{h_{d,1}}, \cdots, \kappa_K\hat{h_{d,K}}]^T \in \mathbb{C}^{K\times 1}$, $\boldsymbol{\Lambda} = [\kappa_1\boldsymbol{\eta}_1, \cdots, \kappa_K\boldsymbol{\eta}_K] \in \mathbb{C}^{M\times K}$, and $\boldsymbol{v} = \boldsymbol{\kappa}\cdot\boldsymbol{t} \in \mathbb{C}^{K\times 1}$.

Then we introduce an auxiliary variable $\boldsymbol{\varphi}$, which is a $K \times 1$ unit-modulus vector containing the phase information of the target beam pattern. The problem $\mathbb{P}$ can be sequentially reformulated as

$$\mathbb{P}1: \min_{\boldsymbol{\theta},\boldsymbol{\varphi}} \quad \|\boldsymbol{V}\boldsymbol{\varphi} - \boldsymbol{u} - \boldsymbol{\Lambda}^H\boldsymbol{\theta}\|_2^2. \tag{9a}$$

$$\text{s.t.} \quad |\theta_m| = 1, m = 1, \cdots, M, \tag{9b}$$

$$|\varphi_k| = 1, k = 1, \cdots, K, \tag{9c}$$

where $\boldsymbol{V} = \text{diag}(\boldsymbol{v})$.

In order to realize the normalization minimization, the two variables $\boldsymbol{\theta}$ and $\boldsymbol{\varphi}$ are optimized iteratively until convergence. Firstly, with fixed RIS passive beamforming $\boldsymbol{\theta}$, $\boldsymbol{\varphi}$ can be

obtained by $\boldsymbol{\varphi} = e^{j\angle(\boldsymbol{u}+\boldsymbol{\Lambda}^H\boldsymbol{\theta})}$ (see proof in [16]). Then, with fixed $\boldsymbol{\varphi}$, we rewrite $\overline{\boldsymbol{v}} = \begin{bmatrix}\mathcal{R}e\{\boldsymbol{V}\boldsymbol{\varphi}-\boldsymbol{u}\}\\ \mathcal{I}m\{\boldsymbol{V}\boldsymbol{\varphi}-\boldsymbol{u}\}\end{bmatrix}$, $\overline{\boldsymbol{\Lambda}} = \begin{bmatrix}\mathcal{R}e\{\boldsymbol{\Lambda}\} & -\mathcal{I}m\{\boldsymbol{\Lambda}\}\\ \mathcal{I}m\{\boldsymbol{\Lambda}\} & \mathcal{R}e\{\boldsymbol{\Lambda}\}\end{bmatrix}$, and $\overline{\boldsymbol{\theta}} = \begin{bmatrix}\mathcal{R}e\{\boldsymbol{\theta}\}\\ \mathcal{I}m\{\boldsymbol{\theta}\}\end{bmatrix}$. The RIS unit modulus weights constraint (9b) can be therefore rewritten as

$$\overline{\theta}_m^2 + \overline{\theta}_{m+M}^2 = 1, \quad m = 1, \cdots, M. \tag{10}$$

Furthermore, we introduce a new auxiliary variable $\boldsymbol{b}$, then the original problem can be transformed into the following form:

$$\mathbb{P}2: \min_{\overline{\boldsymbol{\theta}}} \quad \|\overline{\boldsymbol{v}} - \overline{\boldsymbol{\Lambda}}^H\overline{\boldsymbol{\theta}}\|_2^2. \tag{11a}$$

$$\text{s.t.} \quad \boldsymbol{b} = \overline{\boldsymbol{\theta}}. \tag{11b}$$

$$b_m^2 + b_{m+M}^2 = 1, \quad m = 1, \cdots, M. \tag{11c}$$

The raised optimization problem can be effectively solved by the ADMM algorithm [17]. Specifically, by introducing a Lagrangian multiplier $\boldsymbol{\lambda} \in \mathbb{C}^{2M\times 1}$, problem $\mathbb{P}2$ can be rephrased as

$$L_\rho(\overline{\boldsymbol{\theta}}, \boldsymbol{b}, \boldsymbol{\lambda}) = \|\overline{\boldsymbol{v}} - \overline{\boldsymbol{\Lambda}}^H\overline{\boldsymbol{\theta}}\|_2^2 + \frac{\rho}{2}\|\boldsymbol{b} - \overline{\boldsymbol{\theta}}\|_2^2 + \boldsymbol{\lambda}^T(\boldsymbol{b} - \overline{\boldsymbol{\theta}}), \tag{12}$$

where $\overline{\boldsymbol{\theta}}$, $\boldsymbol{b}$, and $\boldsymbol{\lambda}$ are updated alternatively. Particularly, in the t-th iteration, $\overline{\boldsymbol{\theta}}$, $\boldsymbol{b}$, and $\boldsymbol{\lambda}$ are updated as

$$\boldsymbol{b}^{(t)} = \arg\min_{(11c)} L_\rho(\overline{\boldsymbol{\theta}}^{(t-1)}, \boldsymbol{b}, \boldsymbol{\lambda}^{(t-1)}), \tag{13}$$

$$\overline{\boldsymbol{\theta}}^{(t)} = \arg\min L_\rho(\overline{\boldsymbol{\theta}}, \boldsymbol{b}^t, \boldsymbol{\lambda}^{(t-1)}), \tag{14}$$

$$\boldsymbol{\lambda}^{(t)} = \boldsymbol{\lambda}^{(t-1)} + \rho(\boldsymbol{b}^{(t)} - \overline{\boldsymbol{\theta}}^{(t)}). \tag{15}$$

Note that the optimization of $\boldsymbol{b}$ is constrained by (11c). By solving (13) and (14), we can get

$$b_{i=\{m,m+M\}}^{(t)} = \frac{\overline{\theta}_i^{(t-1)} + (1/\rho)\lambda_i^{(t-1)}}{\sqrt{(\overline{\theta}_m^{(t-1)} + (1/\rho)\lambda_m^{(t-1)})^2 + (\overline{\theta}_{m+M}^{(t-1)} + (1/\rho)\lambda_{m+M}^{(t-1)})^2}}, \tag{16}$$

$$\overline{\boldsymbol{\theta}}^{(t)} = (\overline{\boldsymbol{\Lambda}}\overline{\boldsymbol{\Lambda}}^T + \rho\boldsymbol{I})^{-1}(\overline{\boldsymbol{\Lambda}}\overline{\boldsymbol{v}} + \rho\boldsymbol{b}^{(t)} - \boldsymbol{\lambda}^{(t-1)}). \tag{17}$$

With updated $\overline{\boldsymbol{\theta}}$, $\boldsymbol{\theta}$ can be recovered, and the phase of the desired pattern can be sequentially obtained by

$$\boldsymbol{\varphi}^{(t)} = e^{j\angle(\boldsymbol{u}+\boldsymbol{\Lambda}^H\boldsymbol{\theta}^{(t)})}. \tag{18}$$

The iterative optimization stops either when the maximum number of iterations or the convergence reaches. In particular, the convergence criterion is [17]

$$\mathcal{C}: \begin{cases} \|\boldsymbol{b}^{(t)} - \overline{\boldsymbol{\theta}}^{(t)}\|_2^2 \le \epsilon_1 \\ \|\rho(\overline{\boldsymbol{\theta}}^{(t)} - \overline{\boldsymbol{\theta}}^{(t-1)})\|_2^2 \le \epsilon_2 \end{cases}. \tag{19}$$

The entire algorithm is summarized in Algorithm 1.

Algorithm 1 Proposed passive beamforming $\boldsymbol{\theta}$ optimization algorithm for pattern synthesis

Input: $\boldsymbol{V}$, $\boldsymbol{u}$, $\boldsymbol{\Lambda}$, $\boldsymbol{\theta}^0$, and $\boldsymbol{\lambda}^0$.
Output: $\boldsymbol{\theta}$, $p_k, k = 1, \cdots, K$.
for $t = 1 : T$ **do**
  Obtain $\boldsymbol{\varphi}$ by (18);
  Update $\overline{\boldsymbol{v}}$, $\overline{\boldsymbol{\Lambda}}$, and $\overline{\boldsymbol{\theta}}$;
  With fixed $\boldsymbol{\theta}^{(t-1)}$ and $\boldsymbol{\lambda}^{(t-1)}$, update $\boldsymbol{b}^{(t)}$ by (16);
  With fixed $\boldsymbol{b}^{(t)}$ and $\boldsymbol{\lambda}^{(t-1)}$, update $\overline{\boldsymbol{\theta}}^{(t)}$ by (17);
  With fixed $\boldsymbol{b}^{(t)}$ and $\overline{\boldsymbol{\theta}}^{(t)}$, update $\boldsymbol{\lambda}^{(t)}$ by (15).
  if $\mathcal{C}$ satisfies **then**
    BREAK
  end if
end for
Obtain $\boldsymbol{\theta}$ by $\theta_m = \overline{\theta}_m + j\overline{\theta}_{m+M}, m = 1, \cdots, M$.
Obtain p_k by (6), where $k = 1, 2, \ldots, K$.

IV. Simulation Results

We consider a BS equipped with a 32-antenna array located at coordinates $(0\text{m}, 0\text{m})$. A single RIS is employed to establish high-quality reflective connections between the BS and users. The angular parameters are set as follows: $\varphi_n = 30°$, $\theta_n = -60°$ for $n = 1, \cdots, N$, and $\varphi_{i,m} = -30°$, $\theta_{i,m} = 60°$ for $m = 1, \cdots, M$. We select K directions in the vicinity of the RIS, covering a radius of 10m. The specific simulation parameters are outlined in Table 1. Notably, the channel path-loss adheres to the 3GPP propagation environment guidelines [18]. The noise power has a spectral density of -170 dBm/Hz. We assume the transmission bandwidth is 200 kHz, and therefore the noise power is about $\sigma_n^2 = -117$ dBm. Furthermore, the rician factor is set as $\varepsilon = 10$.

TABLE I: Simulation Parameters.

Parameters	Values
BS location	(0m,0m)
RIS location	(1000m,0m)
Path-loss for $\boldsymbol{G}$ and $\boldsymbol{h}_{r,l}$ (in dB)	$35.6 + 22.0lg(d)$
Path-loss for $\boldsymbol{H_d}$ (in dB)	$32.6 + 36.7lg(d)$
Transmit power	30 dBm
Noise power	-117 dBm

Fig. 2 demonstrates the convergence of our proposed algorithm under the different number of RIS elements. It can be seen that the objective function decreases rapidly at initial, and converges to a stable value within limited iterations, revealing good convergence behaviour of the proposed ADMM algorithm. Additionally, it can be discovered that the RIS comprising more elements results in a smaller objective function value, representing a better match between the optimized and target beam pattern.

In Fig. 3, we study the comparison between the target and optimized power pattern by our proposed algorithm under different numbers of illumination and null areas. A RIS with 180 elements is applied. In detail, we set $Q = \{1, 2\}$ and $R = \{1, 2\}$. In order to illustrate the suppression within the null spaces, the weighting factor within the null areas are set as $\kappa_k = 1000, k \in K_R$, while the weighting factor at other directions are set as 1. To evaluate the matching between the actual and target pattern at the null and illumination areas, we introduce the measurement indicator ι, which is defined as $\iota = \|\hat{\boldsymbol{t}} - \hat{\boldsymbol{p}}\|_2$, where $\hat{\boldsymbol{t}} = \boldsymbol{t}(K_Q, K_R)$, $\hat{\boldsymbol{p}} = \boldsymbol{p}(K_Q, K_R)$. Then,

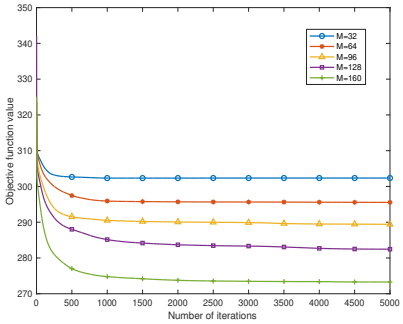

Fig. 2: The convergence behaviour of the proposed algorithm.

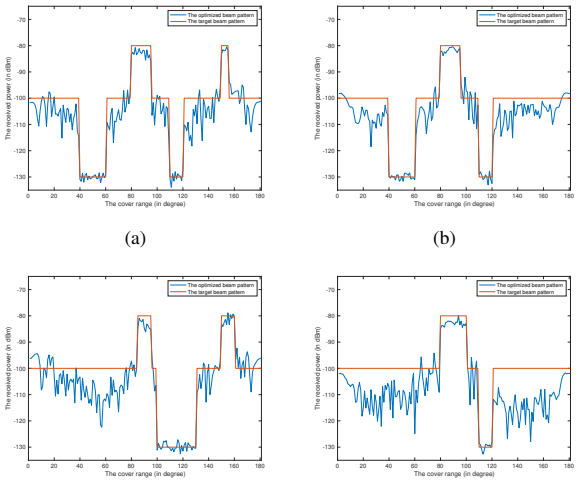

(a) (b)

(c) (d)

Fig. 3: The comparison between the target and optimized power pattern: (a) Q=2; R=2. (b) Q=1; R=2. (c) Q=2; R=1. (d) Q=1; R=1.

ι for the four cases are 16.06, 10.50, 16.85, and 14.88 dB, respectively. It can be seen that the optimized power pattern always matches well with the target pattern with the minimized deviation. Our proposed algorithm is robust against different number and size of both illumination and null areas.

V. Conclusion

In this paper, we propose a RIS-aided joint wide illumination and null insertion design. The study of the joint wide illumination and null design in RIS-aided systems is crucial, as the accurate CSI is not required to cover the target region, and at the same time signals are suppressed towards unwanted regions. Specifically, we propose an optimization problem to minimize the deviation between the desired and actual power patterns, given constraint of the unit modulus weight of each RIS element. To address the non-convexity, an ADMM-based algorithm is proposed, which formulate a Lagrangian function enabling the optimized RIS phase shifts within finite update iterations. Simulation results prove the convergence of our proposed algorithm and demonstrate the good match between the target and optimized power pattern.

References

[1] Q. Wu and R. Zhang, "Towards Smart and Reconfigurable Environment: Intelligent Reflecting Surface Aided Wireless Network," *IEEE Communications Magazine*, vol. 58, no. 1, pp. 106–112, 2020.

[2] M. Dunna, C. Zhang, D. Sievenpiper, and D. Bharadia, "ScatterMIMO: Enabling Virtual MIMO with Smart Surfaces," in *Proceedings of the 26th Annual International Conference on Mobile Computing and Networking*, ser. MobiCom '20. New York, NY, USA: Association for Computing Machinery, 2020. [Online]. Available: https://doi.org/10.1145/3372224.3380887

[3] Ö. Özdogan, E. Björnson, and E. G. Larsson, "Intelligent reflecting surfaces: Physics, propagation, and pathloss modeling," *IEEE Wireless Communications Letters*, vol. 9, no. 5, pp. 581–585, 2019.

[4] D. Zhao, H. Lu, Y. Wang, H. Sun, and Y. Gui, "Joint Power Allocation and User Association Optimization for IRS-Assisted mmWave Systems," *IEEE Transactions on Wireless Communications*, vol. 21, no. 1, pp. 577–590, 2022.

[5] J. Rains, J. ur Rehman Kazim, A. Tukmanov, L. Zhang, Q. H. Abbasi, and M. A. Imran, *Practical Design Considerations for Reconfigurable Intelligent Surfaces*, 2023, pp. 99–122.

[6] X. Yuan, W. Li, Y. Hu, and A. Schmeink, "Beamforming Design and Resource Allocation for IRS-Assisted NOMA Cognitive Radio System," in *2022 International Symposium on Wireless Communication Systems (ISWCS)*, 2022, pp. 1–6.

[7] W. Zhang and W. Wang, "IRS-aided Indoor Millimeter-wave System: Near-field Codebook Design," in *2022 IEEE Globecom Workshops (GC Wkshps)*, 2022, pp. 1489–1494.

[8] K. Singh, P.-C. Wang, S. Biswas, S. K. Singh, S. Mumtaz, and C.-P. Li, "Joint Active and Passive Beamforming Design for RIS-Aided IBFD IoT Communications: QoS and Power Efficiency Considerations," *IEEE Transactions on Consumer Electronics*, vol. 69, no. 2, pp. 170–182, 2023.

[9] M. He, J. Xu, W. Xu, H. Shen, N. Wang, and C. Zhao, "RIS-Assisted Quasi-Static Broad Coverage for Wideband mmWave Massive MIMO Systems," *IEEE Transactions on Wireless Communications*, vol. 22, no. 4, pp. 2551–2565, 2023.

[10] V. Jamali, G. C. Alexandropoulos, R. Schober, and H. V. Poor, "Low-to-Zero-Overhead IRS Reconfiguration: Decoupling Illumination and Channel Estimation," *IEEE Communications Letters*, vol. 26, no. 4, pp. 932–936, 2022.

[11] P. Callaghan and P. R. Young, "Beam- and Band-Width Broadening of Intelligent Reflecting Surfaces Using Elliptical Phase Distribution," *IEEE Transactions on Antennas and Propagation*, vol. 70, no. 10, pp. 8825–8832, 2022.

[12] M. F. Fernández and K.-B. Yu, "Blocking-matrix and quasimatrix techniques for extended-null insertion in antenna pattern synthesis," in *2015 IEEE Radar Conference (RadarCon)*, 2015, pp. 0198–0203.

[13] K.-B. Yu and M. F. Fernández, "Antenna pattern synthesis with multiple discrete and continuous nulls," in *IET International Radar Conference 2015*, 2015, pp. 1–7.

[14] Y.-K. Li and A. Petropulu, "Efficient Beamforming Designs for IRS-Aided DFRC Systems," in *2023 24th International Conference on Digital Signal Processing (DSP)*, 2023, pp. 1–5.

[15] J. Tranter, N. D. Sidiropoulos, X. Fu, and A. Swami, "Fast Unit-Modulus Least Squares With Applications in Beamforming," *IEEE Transactions on Signal Processing*, vol. 65, no. 11, pp. 2875–2887, 2017.

[16] Y. Liu, B. Jiu, and H. Liu, "Admm-based Transmit Beampattern Synthesis for Antenna Arrays Under a Constant Modulus Constraint," *Signal Processing*, vol. 171, p. 107529, 2020.

[17] S. Boyd, N. Parikh, E. Chu, B. Peleato, J. Eckstein *et al.*, "Distributed Optimization and Statistical Learning via the Alternating Direction Method of Multipliers," *Foundations and Trends® in Machine learning*, vol. 3, no. 1, pp. 1–122, 2011.

[18] H. Guo, Y.-C. Liang, J. Chen, and E. G. Larsson, "Weighted Sum-Rate Maximization for Reconfigurable Intelligent Surface Aided Wireless Networks," *IEEE Transactions on Wireless Communications*, vol. 19, no. 5, pp. 3064–3076, 2020.